ELSEVIER

www.elsevier.nl/locate/jorganchem

Journal of Organometallic Chemistry 611 (2000) 386–391

Journal of Organometallic Chemistry

Formation of μ_4-Se_2 complex by the oxidative coupling of μ-SeH complex: double-site atomic inversion of the μ_4-Se_2 complex $[\{(Cp^*Rh)_2(\mu\text{-}CH_2)_2\}_2(\mu_4\text{-}Se_2)]^{2+}$ ($Cp^* = \eta^5\text{-}C_5Me_5$)

Hiroshi Shimomura [b], Takanori Nishioka [a], Masaaki Abe [c], Isamu Kinoshita [a], Kiyoshi Isobe [a,*]

[a] *Department of Material Science, Graduate School of Science, Osaka City University 3-3-138 Sugimoto, Sumiyoshi-ku, Osaka 558-8585, Japan*
[b] *Department of Chemistry, Joetsu University of Education, Jouetu, Niigata 843-8512, Japan*
[c] *Division of Chemistry, Graduate School of Science, Hokkaido University, Sapporo 060-0810, Japan*

Received 22 February 2000; accepted 3 April 2000

Abstract

A reaction of *trans*-$[(Cp^*Rh)_2(\mu\text{-}CH_2)_2Cl_2]$ with H_2Se in MeOH formed a μ-SeH complex isolated as a BPh_4 salt $[(Cp^*Rh)_2(\mu\text{-}CH_2)_2(\mu\text{-}SeH)](BPh_4)$ (**1**; $Cp^* = \eta^5\text{-}C_5Me_5$). In solution, complex **1** was oxidized by molecular oxygen giving a tetranuclear diselenide μ_4-Se_2 complex $[\{(Cp^*Rh)_2(\mu\text{-}CH_2)_2\}_2(\mu_4\text{-}Se_2)](BPh_4)_2$ (**2**). The structure involves Se_2 bridging two Rh–Rh bonds (Rh–Rh = 2.6353(5) Å) in a side-on fashion (Rh(1)–Se(1) = 2.4715(6), Rh(2)–Se(1)* = 2.5526(6) Å). The Se(1)–Se(1)* distance is 2.3875(9) Å, which corresponds to a Se–Se single bond. Complex **2** showed an intriguing dynamic behavior of double-site atomic inversion at the selenium atoms in CD_3CN. The line shape analyses of the temperature dependent ^{1}H-NMR spectra of the μ-CH_2 groups elucidated the dynamic process and provided the activation parameters: $\Delta H^{\ddagger} = 70 \pm 1$ kJ mol^{-1}, $\Delta S^{\ddagger} = 15 \pm 5$ J mol^{-1} K^{-1}, and $\Delta G^{\ddagger} = 66 \pm 1$ kJ mol^{-1} (at 298 K).

Keywords: Hydroselenide complex; Tetranuclear complex; Diselenide complex; Double-site inversion; Line-shape analysis; Rh–Rh bond

1. Introduction

Diselenide complexes have been synthesized using M_2Se_2 (M = Na or Li) [1], red or gray Se [2], polyselenides [1a,3], or H_2Se [4]. Even though a small number of hydroselenide complexes have been isolated [2b,d,f,4d], to our knowledge, there is no direct evidence for the formation of diselenide complexes from the oxidative coupling of hydroselenide complexes.

In order to synthesize diselenide complexes from hydroselenide complexes, a μ-SeH rhodium complex was prepared by a method similar to that for the μ-SH complex, which was synthesized by our group several years ago [5,6]. Furthermore, the reactivity of the μ-SeH complex towards oxidation was compared with that of the μ-SH complex, which is not oxidized by oxygen or a strong oxidant, such as Ag^+ in CH_2Cl_2 [7]. Herein, the preparation of the μ-SeH analog $[(Cp^*Rh)_2(\mu\text{-}CH_2)_2(\mu\text{-}SeH)]^+$ and its oxidation to a diselenide complex $[\{(Cp^*Rh)_2(\mu\text{-}CH_2)_2\}_2(\mu_4\text{-}Se_2)]^{2+}$ by the oxidative coupling of the μ-SeH group are reported [8]. Finally, evidence for a double-site inversion [9] involving the diselenide complex is presented.

2. Results and discussion

2.1. Synthesis and ^{1}H-NMR spectral data of the μ-SeH complex **1** and μ_4-Se_2 complex **2**

The μ-SeH complex $[(Cp^*Rh)_2(\mu\text{-}CH_2)_2(\mu\text{-}SeH)](BPh_4)$ (**1**) was prepared similarly to the μ-SH complex $[(Cp^*Rh)_2(\mu\text{-}CH_2)_2(\mu\text{-}SH)](BPh_4)$ [5]. H_2Se gas was bubbled into a brown suspension of *trans*-$[(Cp^*Rh)_2(\mu\text{-}CH_2)_2Cl_2]$ [10] in CH_3OH at room temperature to rapidly form a reddish–brown solution. To the solution, $NaBPh_4$ in CH_3OH was added to give red-

* Corresponding author. Fax: +81-6-66902753.
E-mail address: isobe@cubane.sci.oska-cu.ac.jp (K. Isobe).

0022-328X/00/$ - see front matter
PII: S0022-328X(00)00474-5

dish–brown crystals of complex **1** in 91% yield. Complex **1** is soluble in halogenated solvents and CH_3CN and is significantly air-sensitive. The ^{1}H-NMR spectrum of **1** in CD_3CN at -30°C shows a signal at δ -4.70, which might be a reasonable chemical shift value for the proton of μ-SeH. There are only a few transition metal complexes with hydroselenide ligands to compare chemical shift values of the SeH groups. $[RhIr(H)(\mu\text{-SeH})(CO)_2(dppm)_2]$ [4d], $[(MeCp)Ru(PPh_3)_2SeH]$ [2b], $[Cp^*_2Ta_2(Se)SeH]$ [2d], and $[Cp'_2Ta_2(H)_2SeH]$ ($Cp' = t$-BuC_5H_4) [2f] have SeH chemical shift values of δ -4.90, -5.74, -3.96, and -4.86, respectively. The four protons of the two μ-CH_2 groups in **1** have different chemical environments due to the stereochemistry of the lone pair of electrons on the Se atom, and appear at δ 7.79, 8.30, 8.56, and 9.00. Above -30°C these signals become broad, which suggests the occurrence of fluxionality resulting from an inversion at the Se atom. A similar fluxionality due to the inversion at the S atom was found in the μ-SH analog $[(Cp^*Rh)_2(\mu\text{-}CH_2)_2(\mu\text{-}SH)](BPh_4)$ [5].

Table 1
Crystallographic data including experimental conditions and refinement of X-ray analysis [a]

Compound	$[\{(RhCp^*)_2(\mu\text{-}CH_2)_2\}_2(\mu_4\text{-}Se_2)](BPh_4)_2 \cdot p\text{-}C_6H_4Me_2 \cdot CH_2Cl_2$
Empirical formula	$C_{101}H_{120}B_2Cl_2Rh_4Se_2$
Formula weight	1996.13
Crystal system	Monoclinic
Space group (number)	$C2/c$ (No. 15)
Unit cell dimensions	
a (Å)	33.337(2)
b (Å)	11.551(2)
c (Å)	27.629(2)
β (°)	120.918(5)
V (Å^3)	9127(1)
Z	4
D_{calc} (Mg cm^{-3})	1.452
μ(Mo–K$_\alpha$) (mm^{-1})	1.610
F(000)	4072.00
Radiation (wave length, λ (Å))	Mo–K$_\alpha$ (0.71069)
Temperature (°C)	23
Absorption corrections method	Empirical Ψ scan [b]
Program for absorption corrections	TEXSAN [c]
Method used in structure solution	Direct method (SIR-92 [d])
Weighting scheme	$w^{-1} = \sigma^2(\lvert F_o\rvert) + (0.02\lvert F_o\rvert)^2$
R [e]	0.039
R_w [f]	0.044
Goodness-of fit [g]	1.19
Scattering factors used	Ref. [h]

[a] Detailed information is available in the supplementary material.
[b] Three sets of ψ scan were employed.
[c] Ref. [16a,b].
[d] Ref. [17].
[e] $R = \Sigma\lvert\lvert F_o\rvert - \lvert F_c\rvert\rvert / \Sigma\lvert F_o\rvert$.
[f] $R_w = (\Sigma\, w(\lvert F_o\rvert - \lvert F_c\rvert)^2 / \Sigma\, w\lvert F_o\rvert^2)^{1/2}$.
[g] $S = (\Sigma\, w(\lvert F_o\rvert - \lvert F_c\rvert)^2)^{1/2} / (n_{data} - n_{par})$.
[h] Ref. [18].

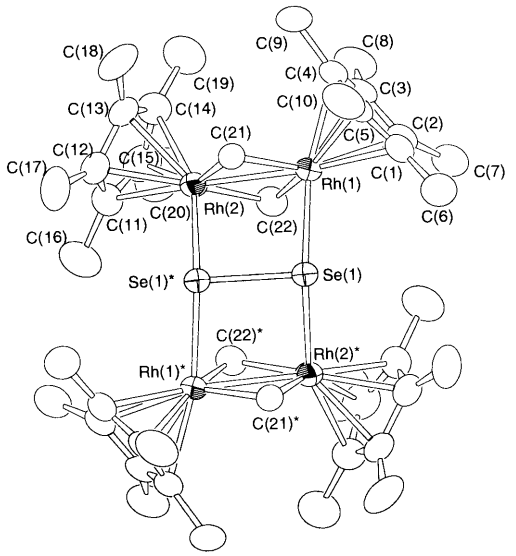

Fig. 1. ORTEP drawing of the cationic moiety of **2** with 50% probability ellipsoids.

Complex **1** in CH_3CN is easily oxidized in air to give the dark brown tetranuclear μ_4-Se_2 complex $[\{(Cp^*Rh)_2(\mu\text{-}CH_2)_2\}_2(\mu_4\text{-}Se_2)](BPh_4)_2$ (**2**) by the oxidative coupling of μ-SeH ligands in 86% yield. On the other hand the μ-SH complex mentioned above is not oxidized to the disulfide complex [5]. The μ_4-SeH group is much more easily oxidized than the μ-SH group. It can be also assumed that the corresponding μ-S_2 complex $[\{(Cp^*Rh)_2(\mu\text{-}CH_2)_2\}_2(\mu_4\text{-}S_2)]^{2+}$ is unstable due to the steric hindrance of the Cp* ligands. To our knowledge, this is the first example of the oxidative coupling of M–SeH fragments to produce a diselenide M_2Se_2 complex. Complex **2** is soluble in CH_3CN, $CHCl_3$, and CH_2Cl_2 and decomposes gradually in air. ^{1}H-NMR spectra of the μ-CH_2 groups in **2** in CD_3CN also show a temperature dependency at higher temperature, and details are mentioned in Section 2.3.

2.2. X-ray structure of the μ_4-Se_2 complex **2**

In order to avoid disorder, which appeared in the $Rh_2Se_2Rh_2$ frame of **2**, p-$C_6H_4Me_2$ was used as a crystallization solvent. Dark brown crystals suitable for X-ray analysis were obtained and crystallographic data are summarized in Table 1. An ORTEP diagram of the cationic part of **2** is shown in Fig. 1. A disorder was still observed in the solvents of crystallization, but it does not effect the structure of **2** itself.

Complex **2** possesses a diselenide ligand bridging the two $\{(Cp^*Rh)_2(\mu\text{-}CH_2)_2\}$ units which are crystallographically related to each other by a two-fold axis passing through the middle point of the Se–Se bond. Within the $\{(Cp^*Rh)_2(\mu\text{-}CH_2)_2\}$ moiety, the bond lengths and angles are all normal and are similar to those found in other methylene bridged dirhodium analogs [5,11]. The Rh–Rh distance (2.6353(5) Å) indicates a Rh–Rh single bond. Since the Se_2 ligand acts as an eight-electron donor, each Rh atom has an 18-electron configuration with the presence of a metal–metal single bond. In this complex, the two Cp* rings are in a staggered conformation [12]. The Se_2 ligand has a formal charge of -2 and is bound to four rhodium atoms. The selected bond lengths, bond angles, and torsion angles are listed in Tables 2–4, respectively. The Rh–Se bond lengths (2.4715(6) and 2.5526(6) Å) indicate that the Se_2 ligand is significantly unsymmetrically bound: this results in a twist of the Rh–Rh bonds from the Se_2 axis as seen in Fig. 2. In addition, the Rh–Se bond lengths are longer than the reported averaged Rh–Se value (2.457(2) Å) [13] for reduction of electron distribution from the Se_2 ligand to each rhodium atom owing to the formation of no less than four Rh–Se bonds. The torsion angle of two Rh–Rh bonds is 26.89°. The observed twisting occurs probably to minimize unfavorable non-bonded contacts between the Cp* groups. The shortest distance between two Cp* ligands is 3.29(1) Å (C(7)–C(16)*). The Se–Se bond length, 2.3875(9) Å, corresponds to an approximate Se–Se single bond according to the bond order-distance correlation proposed by Dahl et al. [2e,3a]. It has been reported that the Se_2 ligand can coordinate to metal ions in various fashions [2a]. In the present system, the Se_2 ligand works as a μ_4,η^4-bridging ligand. The μ_4,η^4-bridging coordination mode has been observed in $[\{SeCo_3(CO)_7\}_2(\mu_4\text{-}Se_2)]$ [2c] which has structure parameters of the $M_2Se_2M_2$ frame similar to those of **2**: the Se–Se bond; 2.3875(9) Å for **2** and 2.352(4) Å for the cobalt diselenide complex: the M–Se–Se bond angle; 88.93(2)–95.04(3)° for **2** and 90.7(2)–93.1(2)° for the cobalt diselenide complex: the dihedral angle between the two planes formed by the diselenide group and the two adjacent metal atoms; 130.08° for **2** and 119° for the cobalt diselenide complex [2c].

Table 2
Selected bond distances (Å) in $[\{(RhCp^*)_2(\mu\text{-}CH_2)_2\}_2(\mu_4\text{-}Se_2)](BPh_4)_2\cdot p\text{-}C_6H_4Me_2\cdot CH_2Cl_2$

Rh(1)–Rh(2)	2.6353(5)	Rh(1)–Se(1)	2.4715(6)
Rh(2)–Se(1) [a]	2.5526(6)	Se(1)–Se(1) [a]	2.3875(9)
Rh(1)–C(1)	2.242(6)	Rh(2)–C(11)	2.208(5)
Rh(1)–C(2)	2.258(5)	Rh(2)–C(12)	2.216(6)
Rh(1)–C(3)	2.280(5)	Rh(2)–C(13)	2.254(5)
Rh(1)–C(4)	2.263(5)	Rh(2)–C(14)	2.245(6)
Rh(1)–C(5)	2.261(5)	Rh(2)–C(15)	2.255(6)
Rh(1)–C(21)	2.047(5)	Rh(2)–C(21)	2.021(5)
Rh(1)–C(22)	2.015(5)	Rh(2)–C(22)	2.072(5)
C(1)–C(2)	1.424(9)	C(11)–C(12)	1.439(9)
C(1)–C(5)	1.415(8)	C(11)–C(15)	1.399(8)
C(1)–C(6)	1.498(9)	C(11)–C(16)	1.507(8)
C(2)–C(3)	1.416(8)	C(12)–C(13)	1.413(8)
C(2)–C(7)	1.506(9)	C(12)–C(17)	1.485(9)
C(3)–C(4)	1.414(8)	C(13)–C(14)	1.417(9)
C(3)–C(8)	1.484(9)	C(13)–C(18)	1.489(9)
C(4)–C(5)	1.439(8)	C(14)–C(15)	1.439(9)
C(4)–C(9)	1.496(7)	C(14)–C(19)	1.500(8)
C(5)–C(10)	1.484(9)	C(15)–C(20)	1.47(1)

[a] Symmetry operation: $-x$, y, $1/2-z$

Table 3
Selected bond angles (°) in $[\{(RhCp^*)_2(\mu\text{-}CH_2)_2\}_2(\mu_4\text{-}Se_2)](BPh_4)_2\cdot p\text{-}C_6H_4Me_2\cdot CH_2Cl_2$

Rh(2)–Rh(1)–Se(1)	85.31(2)	Rh(1)–Rh(2)–Se(1) [a]	87.38(2)
Rh(1)–Se(1)–Rh(2) [a]	132.25(3)		
Rh(1)–Se(1)–Se(1) [a]	95.04(3)	Rh(2) [a]–Se(1)–Se(1) [a]	88.93(2)
Rh(2)–Rh(1)–C(21)	49.2(1)	Rh(1)–Rh(2)–C(21)	50.0(1)
Rh(2)–Rh(1)–C(22)	50.8(1)	Rh(1)–Rh(2)–C(22)	48.9(1)
C(21)–Rh(1)–C(22)	100.0(2)	C(21)–Rh(2)–C(22)	98.9(2)
Rh(1)–C(21)–Rh(2)	80.8(2)	Rh(1)–C(22)–Rh(2)	80.3(2)
C(2)–C(1)–C(5)	108.4(6)	C(1)–C(2)–C(3)	108.5(6)
C(2)–C(1)–C(6)	126.8(7)	C(1)–C(2)–C(7)	126.5(7)
C(5)–C(1)–C(6)	124.5(7)	C(3)–C(2)–C(7)	123.5(7)
C(2)–C(3)–C(4)	107.4(6)	C(3)–C(4)–C(5)	108.8(5)
C(2)–C(3)–C(8)	124.7(6)	C(3)–C(4)–C(9)	125.6(5)
C(4)–C(3)–C(8)	127.6(6)	C(5)–C(4)–C(9)	124.8(5)
C(1)–C(5)–C(4)	106.8(5)	C(1)–C(5)–C(10)	126.0(6)
C(4)–C(5)–C(10)	127.0(6)		
C(12)–C(11)–C(15)	109.0(5)	C(11)–C(12)–C(13)	107.1(5)
C(12)–C(11)–C(16)	124.5(6)	C(11)–C(12)–C(17)	126.5(6)
C(15)–C(11)–C(16)	126.2(7)	C(13)–C(12)–C(17)	126.2(7)
C(12)–C(13)–C(14)	108.6(6)	C(13)–C(14)–C(15)	107.9(5)
C(12)–C(13)–C(18)	125.7(7)	C(13)–C(14)–C(19)	127.3(7)
C(14)–C(13)–C(18)	125.5(6)	C(15)–C(14)–C(19)	124.0(7)
C(11)–C(15)–C(14)	107.4(6)	C(11)–C(15)–C(20)	127.2(7)
C(14)–C(15)–C(20)	125.1(7)		

[a] Symmetry operation: $-x$, y, $1/2-z$

2.3. Dynamic process of the μ_4-Se_2 complex **2**

Variable-temperature ^{1}H-NMR spectroscopy indicates that complex **2** is fluxional in CD_3CN. Line-shape

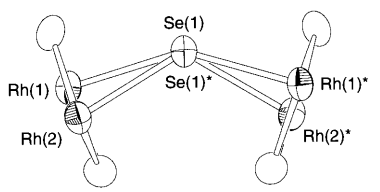

Fig. 2. Side view down the Se–Se bonds of the Rh_4Se_2 framework of **2** showing the conformation of the Rh–Rh bonds relative to the Se–Se axis.

Table 4
Selected torsion angles (°) in $[\{(RhCp^*)_2(\mu\text{-}CH_2)_2\}_2(\mu_4\text{-}Se_2)](BPh_4)_2 \cdot p\text{-}C_6H_4Me_2 \cdot CH_2Cl_2$

(1)	(2)	(3)	(4)	Angle [b]	(1)	(2)	(3)	(4)	Angle [b]
Rh(1)	Rh(2)	Se(1) [a]	Se(1)	−13.51(2)	Rh(1)	Se(1)	Se(1) [a]	Rh(1) [a]	146.80(3)
Rh(1)	C(21)	Rh(2)	C(22)	2.5(2)	Rh(2)	Se(1) [a]	Se(1)	Rh(2) [a]	−117.87(3)
Rh(2)	Rh(1)	Se(1)	Se(1) [a]	−14.04(1)	Rh(2)	C(21)	Rh(1)	C(22)	−2.5(2)
Rh(2)	C(22)	Rh(1)	C(21)	2.5(2)	C(21)	Rh(1)	Rh(2)	C(22)	−176.8(3)
C(21)	Rh(2)	Rh(1)	C(22)	176.8(3)					

[a] Symmetry operation: $-x, y, 1/2-z$.
[b] The sign is positive, if when looking from atom 2 to atom 3 a clock-wise motion of atom 1 would superimpose it on atom 4.

analysis of the ^{1}H-NMR signals of μ-CH_2 for **2** was carried out using the spectrum measured at −30°C as the low temperature limit spectrum. Two specific sets of μ-CH_2 resonances were determined by trial and error until the observed spectra, with a given rate constant, were reproducible in the entire temperature range (30–80°C). The two sets of singlets, δ 9.27 (A) and 9.65 (C); δ 9.37 (B) and 10.12 (D), were taken as the exchange couples (see left side of Fig. 3).

Due to the existence of the two-fold axis passing through the middle point of the Se–Se bond, **2** shows four singlets of the μ-CH_2 ligands at δ 9.27 (A), 9.37 (B), 9.65 (C), and 10.12 (D) with equal intensity at 30°C. The full assignment of these four signals to each proton was not attained. These chemically unequivalent protons in the $\{(Cp^*Rh)_2(\mu\text{-}CH_2)_2\}$ moiety indicate no inversion operation at the selenium centers at 30°C. However, at higher temperatures these signals show a temperature-dependency in CD_3CN as displayed on the left hand-side of Fig. 3: with increasing temperature, line broadening becomes evident at about 40°C, and as the temperature increases further, resonances A and C merge first into a singlet peak at δ ca. 9.4 over 55°C. At temperatures over 70°C resonances B and D merge into a singlet peak at δ ca. 9.7. This averaging process is fully reversible.

This process at higher temperatures can be explained by assuming the occurrence of inversion at the selenium atoms, and may be attributed to two-site exchange processes with equally populated, uncoupled sites [14]. Calculated spectra and rate constants are shown on the right hand-side of Fig. 3. Fig. 4 shows the Eyring plots which yield $\Delta H^{\ddagger} = 70 \pm 1$ kJ mol^{-1}, $\Delta S^{\ddagger} = 15 \pm 5$ J mol^{-1} K^{-1}, and $\Delta G^{\ddagger} = 66 \pm 1$ kJ mol^{-1} (at 298 K). The small entropic contribution strongly suggests that the exchange process is an intramolecular inversion that proceeds through a trigonal-planar transition state of the Se centers [15]. The $\Delta G^{\ddagger}$ value (66 ± 1 kJ mol^{-1}), being higher than those of the usual single-site inversion (in most cases ca. 50 kJ mol^{-1}), is clearly associated with an appreciably slower inversion of the selenium atom pair [9,15]. It was suggested that in some complexes with organic diselenide ligands such as $[(PtXMe_3)_2(MeSeSeMe)]$ [9a], $[Re_2X_2(CO)_6(RCH_2SeSeCH_2R)]$ [9b], and $[(PtXMe_3)_2(\overline{SeCH_2C(Me)_2CH_2Se})]$ (X = halogen) [9d], synchronous double-site atomic inversion operates as one of the fluxional processes. The

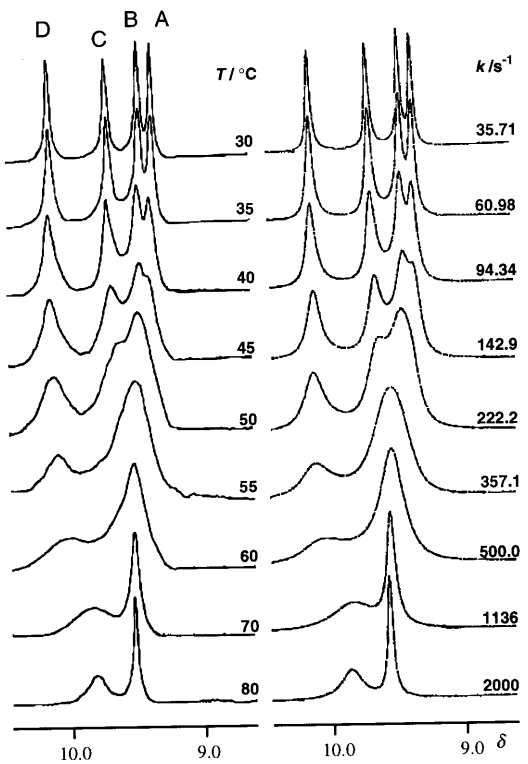

Fig. 3. Observed (left) and calculated (right) ^{1}H-NMR spectra of the μ-CH_2 protons in **2** in CD_3CN.

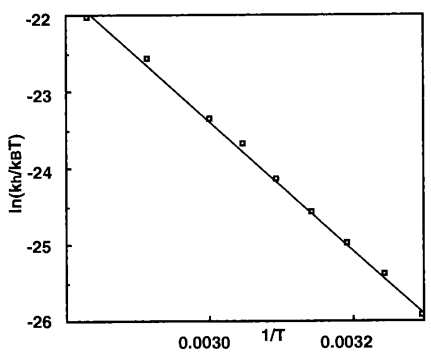

Fig. 4. Eyring plot for double-site atomic inversion of Se_2 in **2**.

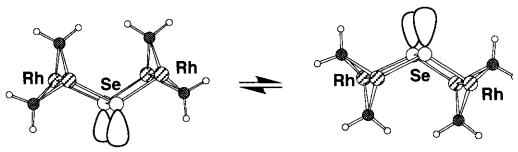

Scheme 1.

last compound consists of a cyclic organic diselenide ligand, and its activation parameters are similar to those of **2**: $\Delta G^{\ddagger}$ values of 74.4 (X = Cl), 74.5 (X = Br), and 74.0 (X = I) kJ mol^{-1} and small $\Delta S^{\ddagger}$ values of -4.0 ± 3.9 (X = Cl), -1.8 ± 2.1 (X = Br), and 0.8 ± 3.3 (X = I) J mol^{-1} K^{-1} [9d]. The fluxionality of **2** can be explained by a similar kind of double-site atomic inversion process, and this process causes flapping of the four-membered rings of Se_2Rh_2 as illustrated in Scheme 1. The flapping motion might be triggered by a synchronous inversion at the two selenium atoms through a transition state with a planar $Rh_2Se_2Rh_2$ moiety. In connection with the transition state, however, at this stage we do not have any evidence for ruling out a non-planar transition state generated by independent double-site inversion.

3. Experimental

The following chemicals were purchased from commercial sources and used without further purification: $RhCl_3 \cdot 3H_2O$ (Shiga Kikinzoku); pentamethylcyclopentadiene (Kanto Kagaku); 15.3% $Al_2(CH_3)_6$ in hexane (Toso Aquzo); Al_2Se_3 (Mitsuwa Kagaku); $Na[B(C_6H_5)_4]$ (Nacalai); CD_3CN (Nacalai); DMF-d_7 (Aldrich); CD_2Cl_2 (Aldrich). Methanol was distilled under argon. The starting compound *trans*-$[(Cp^*Rh)_2(\mu\text{-}CH_2)_2Cl_2]$ was prepared by the reeported literature method [10]. Elemental analyses were performed by the IMS Chemical Material Center and the Chemical Analysis Service Laboratory in Osaka City University. Infrared spectra were recorded on a Hitachi 270-30 spectrometer. Fast atom bombardment (FAB) mass spectra for positive ions using a glycerol matrix were measured on a Shimadzu/Kratos-Concept 1S spectrometer. ^{1}H- and $^{13}C\{^1H\}$-NMR spectra were recorded on a JEOL GX-400 FT-NMR spectrometer.

3.1. Synthesis of the μ-SeH complex *1*

Since complex **1** is significantly air-sensitive, all manipulations were performed under argon. Hydrogen selenide was generated from 3.50 g of aluminum selenide with 20 cm^3 of water. Excess hydrogen selenide was trapped by a 10% aqueous sodium hydroxide solution. Into a suspension of *trans*-$[(Cp^*Rh)_2(\mu\text{-}CH_2)_2Cl_2]$ (0.60 g, 1.00 mmol) in methanol (25 cm^3), hydrogen selenide was bubbled for 45 min at a rate of one bubble per second at room temperature, producing a reddish–brown solution. After purging excess H_2Se with argon, a methanol solution (15 cm^3) of $NaBPh_4$ (3.40 g, 9.94 mmol) was added to the reddish–brown solution, which was then stirred for a further 5 min. The resulting brown crystals were collected by filtration, washed with methanol (10 cm^3), and dried under vacuum (0.82 g, 0.91 mmol, yield 91%). ^{1}H-NMR (CD_3CN, −30°C): δ −4.70 (s, 1H, μ-SeH), δ 1.82 (s, 30H, Me), 7.79 (s, 1H, μ-CH_2), 8.30 (s, 1H, μ-CH_2), 8.56 (s, 1H, μ-CH_2) and 9.00 (s, 1H, μ-CH_2). Anal. Cal. for $C_{46}H_{55}BRh_2Se$: C, 61.15; H, 6.14. Found: C, 60.83; H, 6.28%.

3.1.1. Synthesis of the μ_4-Se_2 complex *2*

A deep brown solution of $[(Cp^*Rh)_2(\mu\text{-}CH_2)_2(\mu\text{-}SeH)](BPh_4)$ (0.80 g, 0.89 mmol) in CH_3CN (50 cm^3) was exposed to air for 8 h with stirring at room temperature. After filtration, toluene (100 cm^3) was added to the filtrate. The solution was concentrated to ca. 10 cm^3 under reduced pressure at 40°C. The resulting dark brown crystals (0.69 g, 0.38 mmol: 86%) were collected, and washed with acetonitrile–toluene. After recrystallization from acetonitrile–toluene, 0.32 g (0.18 mmol: 40%) of dark brown crystals were obtained. On recrystallization, the decomposition products were formed in a small amount. FAB-MS: Calc. for $C_{44}H_{68}S_{e2}Rh_4$: 1167 (the most abundant mass ion). Found: m/z 1167 [M$^+$]. ^{1}H-NMR (CD_3CN, 30°C): δ 1.72 (s, 30H, Me), 9.27 (s, 1H, μ-CH_2), 9.37 (s, 1H, μ-CH_2), 9.65 (s, 1H, μ-CH_2) and 10.12 (s, 1H, μ-CH_2). $^{13}C\{^1H\}$-NMR (CD_3CN): δ 10.34 (s, Me), 104.33 (s, C_5Me_5), 179.00 (s(br), μ-CH_2), 181.00 (s(br), μ-CH_2). Anal. Calc. for $C_{92}H_{108}B_2Rh_4Se_2$: C, 61.22; H, 6.03. Found: C, 60.91; H, 6.22%.

3.2. X-ray structure determination of the μ_4-Se_2 complex *2*

Dark brown crystals suitable for X-ray analysis were grown by slow diffusion of *p*-xylene to the solution of **2** in dichloromethane. A crystal was shielded in a glass capillary. The reflection data were collected by the ω scan technique on an automated four-circle diffractometer Rigaku AFC-7S at 23°C. The unit cell dimensions were determined by a least-squares method using 25 reflections ($29.08 < 2\theta < 29.97°$). Three standard reflections were recorded at regular intervals, and they showed 2.48% decay throughout the data collection. The intensities were corrected for Lorentz and polarization factors, absorption, and decay. An empirical absorption correction was applied by use of ψ scan data. A linear method for decay corrections was employed.

The space group was confirmed by the monoclinic diffraction symmetry, the systematic absences (hkl: $h+k \neq 2n$; $h0l$: $l \neq 0$), and the successful solution and refinement of the structure.

Crystal data for $[\{(Cp^*Rh)_2(\mu\text{-}CH_2)_2\}_2(\mu_4\text{-}Se_2)](BPh_4)_2 \cdot p\text{-}C_6H_4Me_2 \cdot CH_2Cl_2$: $C_{101}H_{120}B_2Cl_2Rh_4Se_2$ (FW = 1996.13), monoclinic, space group $C2/c$ (No. 15), $a = 33.337(2)$, $b = 11.551(2)$, $c = 27.629(2)$ Å, $\beta = 120.918(5)°$, $V = 9127(1)$ Å^3, $Z = 4$, $D_{calc} = 1.452$ g·cm^{-3}, $\mu(Mo\text{–}K_\alpha) = 16.10$ cm^{-1}, crystal size $0.25 \times 0.03 \times 0.70$ mm. The full-matrix refinements of 546 least-squares parameters for all non-hydrogen atoms and 6244 reflections converged at R (R_w) = 0.039 (0.044). A complete lists of bond lengths and angles, hydrogen atom coordinates and anisotropic thermal parameters have been deposited at the Cambridge Crystallographic Data Centre (No. CCDC 143824).

3.3. Line-shape analysis of variable-temperature ^{1}H-NMR spectra of the μ_4-Se_2 complex **2**

Complex **2** (10 mg) was dissolved in CD_3CN (0.7 cm^3). The variable-temperature ^{1}H-NMR measurement was performed on a JEOL GX-400 spectrometer equipped with a standard valuable temperature accessory. Line-shape analysis of variable-temperature ^{1}H-NMR spectra for complex **2** was carried out using a computer program based on a modified Bloch equation with the two-site exchange model [14]. Rate constants were determined by visual fitting of observed and calculated spectra of the μ-CH_2 signals. Activation parameters were calculated from the Eyring plots.

4. Supplementary material

Crystallographic data for the structural analysis has been deposited with the Cambridge Crystallographic Data Centre, CCDC 143824 for compound **2**. Copies of this information may be obtained free of charge from: The Director, CCDC, 12 Union Road, Cambridge, CB2 1EZ, UK (Fax: +44-1223-336-033; e-mail: deposit@ccdc.cam.ac.uk or www: http://www.ccdc.cam.ac.uk).

Acknowledgements

This work was financially supported in part by a Grant-in-Aid for Scientific Research on Priority Areas (No. 09239104) from the Ministry of Education, Science, and Culture, Japan. Thanks are due to the IMS Chemical Material Center and the Chemical Analysis Service Laboratory in Osaka City University for the elemental analyses, MS measurement, and the use of NMR instruments. We also thank to Dr B. Breedlove (a JSPS Postdoctoral Fellow) for his kind reviewing of this paper.

References

[1] (a) D.M. Giolando, M. Papavassiliou, J. Pickardt, T.B. Rauchfuss, R. Steudel, Inorg. Chem. 27 (1988) 2596. (b) S.-P. Huang, M.G. Kanatzidis, Inorg. Chem. 30 (1991) 3572. (c) S. Ryu, D. Whang, H.-J. Kim, K. Kim, M. Yoshida, K. Hashimoto, K. Tatsumi, Inorg. Chem. 36 (1997) 4607.

[2] (a) M.A. Ansari, J.A. Ibers, Coord. Chem. Rev. 100 (1990) 223. (b) J. Amarasekera, E.J. Houser, T.B. Rauchfuss, C.L. Stern, Inorg. Chem. 31 (1992) 1614. (c) G. Gervasio, S.F.A. Kettle, F. Musso, R. Rossetti, P.L. Stanghellini, Inorg. Chem. 34 (1995) 298. (d) J.H. Shin, G. Parkin, Organometallics 14 (1995) 1104. (e) S. Inomata, T. Hiruma, H. Ogino, Chem. Lett. (1998) 309. (f) H. Brunner, M.M. Kubicki, J.-C. Leblanc, W. Meier, C. Moise, A. Sadorge, B. Stubenhofer, J. Wachter, R. Wanninger, Eur. J. Inorg. Chem. (1999) 843. (g) J. Mizutani, K. Matsumoto, Chem. Lett. (2000) 72.

[3] (a) C.F. Campana, F.Y.-K. Lo, L.F. Dahl, Inorg. Chem. 18 (1979) 3060. (b) C. Ratti, P. Richard, A. Tabard, R. Guilard, J. Chem. Soc. Chem. Commun. (1989) 69. (c) R. Guilard, C. Ratti, A. Tabard, P. Richard, D. Dubois, K.M. Kadish, Inorg. Chem. 29 (1990) 2532. (d) M. Herberhold, M. Kuhnlein, M. Schrepfermann, M.L. Ziegler, B. Nuber, J. Organomet. Chem. 398 (1990) 259. (e) L.C. Roof, J.W. Kolis, Chem. Rev. 93 (1993) 1037.

[4] (a) C.M. Bolinger, T.B. Rauchfuss, A.L. Reingold, Organometallics 1 (1982) 1551. (b) A.L. Rheingold, C.M. Bolinger, T.B. Rauchfuss, Acta Crystallogr. Sect. C 42 (1986) 1878. (c) F. Bottomley, R.W. Day, Organometallics 10 (1991) 2560. (d) R. McDonald, M. Cowie, Inorg. Chem. 32 (1993) 1671.

[5] Y. Ozawa, A. Vazquez de Miguel, K. Isobe, J. Organomet. Chem. 433 (1992) 183.

[6] K. Isobe, Y. Ozawa, A. Vazquez de Miguel, T.-W. Zhu, K.-M. Zhao, T. Nishioka, T. Ogura, T. Kitagawa, Angew. Chem. Int. Ed. Engl. 33 (1994) 1882.

[7] T. Nishioka, V.Y. Kukushkin, K. Isobe, A. Vazquez de Miguel, Inorg. Chem. 33 (1994) 2501.

[8] In the presence of excess H_2Se the μ-SeH complex $[(Cp^*Rh)_2(\mu\text{-}CH_2)_2(\mu\text{-}SeH)]^+$ is oxidized by O_2 to afford a tetraselenide complex $[\{(Cp^*Rh)_2(\mu\text{-}CH_2)_2\}_2(\mu_4\text{-}Se_4)]^{2+}$ which will be reported elsewhere.

[9] (a) E.W. Abel, A.R. Khan, K. Kite, K.G. Orrell, V. Sik, J. Chem. Soc. Dalton Trans. (1980) 2220. (b) E.W. Abel, S.K. Bhargava, M.M. Bhatti, M.A. Mazid, K.G. Orrell, V. Sik, M. B. Hursthouse, K.M.A. Malik, J. Organomet. Chem. 250 (1983) 373. (c) E.W. Abel, P.K. Mittal, K.G. Orrell, V. Sik, T.S. Cameron, J. Chem. Soc. Chem. Commun. (1984) 1312. (d) E.W. Abel, P.K. Mittal, K.G. Orrell, V. Sik, J. Chem. Soc. Dalton Trans. (1986) 961.

[10] K. Isobe, S. Okeya, N.J. Meanwell, A.J. Smith, H. Adams, P.M. Maitlis, J. Chem. Soc. Dalton Trans. (1984) 1215.

[11] T. Nishioka, S. Nakamura, Y. Kaneko, T. Suzuki, I. Kinoshita, S. Kiyooka K. Isobe, Chem. Lett. (1996) 911.

[12] D.W. Hoard, P.R. Sharp, Inorg. Chem. 32 (1993) 612.

[13] A.G. Orpen, L. Brammer, F.H. Allen, O. Kennard, D.G. Watson, R. Taylor, J. Chem. Soc. Dalton Trans. (1989) S1.

[14] J. Sandström, Dynamic NMR Spectroscopy, Academic Press, New York, 1982, pp. 18–25.

[15] E.W. Abel, S.K. Bhargava, K.G. Orrell, Prog. Inorg. Chem. 32 (1984) 1.

[16] (a) Molecular Structure Corporation, 1995, TEXSAN, Single Crystal Structure Analysis Software, Version 1.7, MSC, 3200 Research Forest Drive, The Woodlands, TX 77381, USA. (b) A.C.T. North, D.C. Phillips, F.S. Mathews, Acta Cryst. Sect. A 24 (1968) 351.

[17] A. Altomare, M.C. Burla, M. Camalli, M. Cascarano, C. Giacovazzo, A. Guagliardi, G. Polidori, J. Appl. Cryst. 27 (1994) 435.

[18] D.T. Cromer, J.T. Waber, International Tables for X-ray Crystallography, vol. 4, Kynoch Press, Birmingham, 1974.